Pressure- and Temperature-Induced Phase Separation Transition in Homopolymer, Block Copolymer, and Protein in Water

Mitsuhiro Shibayama, Noboru Osaka*

Summary: Effects of temperature, *T*, and pressure, *P*, on phase behavior and structure are discussed on three types of polymeric systems, i.e., a homopolymer (HP), a block copolymer (BC), and a protein (PR) in water. Due to the presence of hydrophobic groups, each system underwent a *T*-induced and *P*-induced phase separation by increasing *T* and *P*, respectively. However, these transitions are different from each other depending on their molecular structures. Small-angle neutron scattering investigations revealed that HP showed a macrophase separation transition (MaST) with respect to both *T* and *P*. BC underwent a microphase separation transition (MiST) followed by a MaST with increasing *T*, while only a MaST was observed with increasing *P*. In the case of PR, on the other hand, *T*-induced and *P*-induced denaturations led to densely-packed aggregates of oligomers and fractal-aggregates of primary particles, respectively. The results from all systems indicated that hydrophobic interactions become insignificant at high pressures.

Keywords: gels; hydrophobic interaction; phase diagram; pressure; small-angle neutron scattering

Introduction

Aqueous solutions of water-soluble polymers carrying hydrophobic groups undergo a phase separation transition at the so-called lower critical solution temperature (LCST). This phase separation transition is due to dehydration of hydrophobic groups on the polymer, i.e., hydrophobic dehydration. Although the hydropobic interaction is one of the key molecular interactions, its understanding is still limited. As a matter of fact, solvation of low molecular-weight compounds (protein prototype) causes a decrease in volume, while protein denaturation is accompanied by a positive volume change. Chalikian and Breslauer discussed this issue as the protein paradox.[1] Kauzmann who proposed the concept of ''hydrophobic bonding'' in 1959 predicted the importance of experiments of hydrophobic interaction as a function of pressure.[2] Investigations of hydrophobic interaction on the molecular level have been extensively carried out by NMR, FTIR, circular dichroism, small-angle X-ray and light scattering, etc. However, the role of hydrostatic pressure on the hydrophobic interaction has not yet been well-elucidated. To rectify this situation, we decided to address first the following simple question: Is the *P*-induced phase separation of polymer aqueous solutions the same as the *T*-induced phase separation? In order to answer this question and explore the origin of hydrophobic interaction, we have been investigating hydrophobic interactions in a unique way. In particular, we employed small-angle neutron scattering (SANS) and investigated phase behaviors near transition thresholds. The structure range covered by SANS is from a few-tens of Ångstrom to a thousand, hence it may not

Institute for Solid State Physics, The University of Tokyo, Kashiwanoha, Kashiwa, Chiba, 277-8581, Japan
Fax: (+81) 4-7134-6069;
E-mail: sibayama@issp.u-tokyo.ac.jp

provide a monomer unit-level understanding of the hydrophobic interaction. However, one can discuss the hydorphobic interaction by way of macrophase (MaST) and microphase separation transition (MiST). We chose three kinds of polymeric systems having different levels of complexity in their molecular structures, i.e., from a homopolymer (HP), to a block copolymer (BC), and to a protein (PR) in aqueous systems, and investigated *T*- and *P*-induced phase separation and/or gelation kinetics.

Experimental Part

Three types of polymeric systems, i.e., HP, BC, and PR, were chosen for pressure-dependent SANS experiments. As for HP, poly(*N*-isopropylacrylamide) (PNIPA) (Scheme 1a) aqueous solutions were prepared with 690 mM of recrystallized *N*-isopropylacrylamide monomer, 1.75 mM of ammonium persulfate, and 8.0 mM of *N*,*N*,*N*',*N*'-tetramethylethylenediamine. A monomer solution in either H_2O or D_2O was degassed and then polymerized in a pressure cell at 20 °C and atomospheric pressure. The second system was a water-soluble and temperature sensitive BC, poly[2-(2-ethoxy)ethoxyethyl vinyl ether]-*block*-poly(2-methoxethyl vinyl ether), (EOEOVE-*b*-PMOVE) (Scheme 1b). EOEOVE-*b*-PMOVE with a narrow molecular weight distribution ($M_n = 5.7 \times 10^4$ Da, $M_w/M_n = 1.28$) was synthesized by living cationic polymerization. The degrees of polymerization were 200 and 400 for PEOEOVE and PMOVE, respectively. The details of the synthesis have been reported elsewhere.[3] At atmospheric pressure, the two constituting homopolymers have lower critical solution temperatures (LCST), PEOEOVE at ca. 40 and PMOVE at ca. 65 °C. The third system is a whey protein, *β*-lactoglobulin (bLG). Crystalized (three times) and lyophilized bLG was purchased from Sigma (lot no. 114H7055). The molecular weight of bLG is 1.84×10^4 Da. Aqueous solutions of bLG were prepared by dissolving the protein in distilled deuterium oxide. The pH of bLG solutions was 7 at ambient pressure.

SANS experiments were carried out at the SANS-U facility of the University of Tokyo located at the JRR-3M reactor guide hall of the Japan Atomic Energy Research Institute. The neutron wavelength was monochromatized to be 7.0 Å with a velocity selector with the wavelength distribution of 10%.[4] Pressure-dependent SANS experiments were conducted using a high-pressure cell, PCI-400-SANS (Syn-Corporation, Co. Ltd. Kyoto, Japan). The PCI-400-SANS is an inner cell-type pressure cell, which was designed to isolate the sample from the pressurizing medium. The basic concept of the pressure cell is described elsewhere.[5] The inner cells have quartz windows of 2 mm thick. The applied pressure is transmitted via a rubber diaphragm connected to the inner cell. The outer chamber was filled with D_2O and the pressure was controlled by pressurising D_2O by a double-cylinder hand pump.

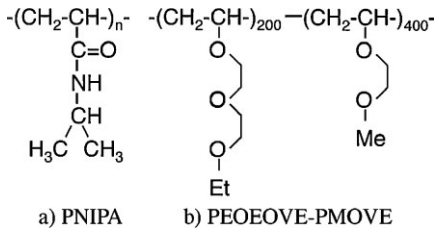

Scheme 1.
Chemical structures of (a) PNIPA and (b) PEOEOVE-*b*-MOVE.

Results and Discussion

Phase Diagram

Figure 1 shows *P*-*T* phase diagrams of (a) PNIPA in H_2O and in D_2O ($C \approx 7$ wt%)[6] and (b) PEOEOVE-*b*-PMOVE in D_2O solutions ($C = 15$ wt%).[7] It is clear from Fig. 1a that the phase diagram has a maximum at around $P = 50$ MPa. Interestingly, such convexity in *P*-*T* phase diagrams is often observed in polymeric systems in aqueous media. Note that there exists an upward shift of about

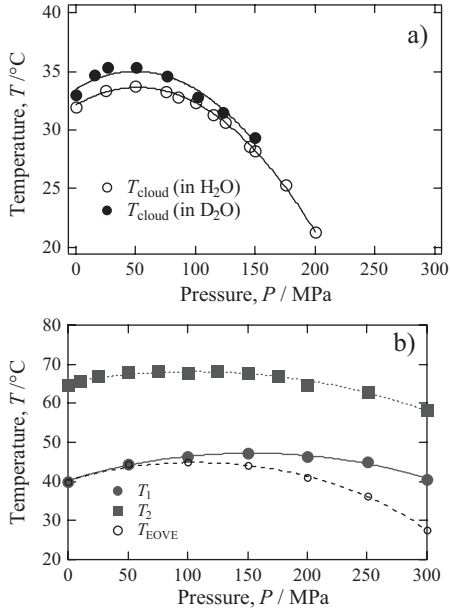

Figure 1.
P-T phase diagrams of (a) PNIPA in H_2O and D_2O, and (b) PEOEOVE-*b*-PMOVE in D_2O.

1.5 °C for the MaST temperature because of the deuteration effect.[8] Fig. 1b shows another example of convexity in a *P-T* phase diagram. This diagram exhibits two transitions, T_1 and T_2, resulting from MiST (transition from a homogeneous solution to a microphase separated structure with a PEOEOVE spherical domain structure) at 40 °C and from MaST at 65 °C (precipitation).[7] It should be noted that the MaST of a PEOEOVE homopolymer solution (shown by the dashed line) is different from the MiST of its block copolymer solution in the high pressure region. This indicates that the MaST of PEOEOVE is more pressure-sensitive than the MiST of PEOEOVE block chains. The reason for the deviation is not clear at this stage and it remains an interesting question for future investigations.

As shown in Fig. 1(a) and (b), convexity in *P-T* phase diagrams is widely observed in aqueous polymer systems.[9] The apical position (P_m, T_m) depends on the kind of polymer. In particular, P_m is dependent on the pressure at which the volume change of mixing, ΔV_m, changes its sign. The details of the convexity are discussed elsewhere.[10] Similar phase diagrams are also observed in protein solutions and regarded as *P*-denaturation and *T*-denaturation, respectively. Hawley regarded such a phase diagram as a part of an elliptical phase diagram and proposed a theory of reversible pressure-temperature denaturation.[11] His theory is extensively reviewed by Smeller.[12] According to the theory, the phase diagram is given by the following Equation for an ellipse,

$$\frac{V_0\Delta\beta}{2\Delta G_0}(P-P_0)^2+\frac{V_0\Delta C_p}{2T_0\Delta G_0}(T-T_0)^2=1 \quad (1)$$

where (P_0, T_0), $\Delta\beta$, and ΔC_p are a reference state, the difference in the isothermal compressibilities, and the heat capacity difference between the one and two phases, respectively. Figure 2 demonstrates an example of an elliptic phase diagram for the PNIPA solution.[6] The data are the same as in Fig. 1a. The center of the ellipse is at (P_0, T_0) = (49.8 MPa, 284 K). ΔG_0 is the free energy at (P_0, T_0). Although a similar phase diagram might be constructed for the BC and the PR, the *P-T* windows for MaST and/or MiST of the experimentally obtained data were too limited for quantiative discussion.

SANS of HP

In order to investigate *T*- and *P*-induced phase separation from the microscopic viewpoint, we carried out SANS experiments.

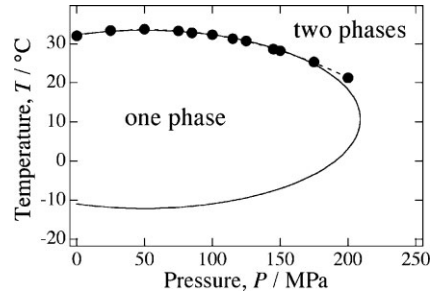

Figure 2.
Elliptic phase diagram for a PNIPA solution (in D_2O). The solid circles denote the data points obtained by experiment.

The SANS intensity functions for semi-dilute polymer solutions are given by the so-called Ornstein-Zernike (OZ) type function,

$$I(q) = \frac{K_{NS}}{v_1}\frac{k_B T\phi^2 N_A}{K_{os}}\frac{1}{1+\xi^2 q^2} \qquad (2)$$

where K_{NS} is the neutron contrast, v_1 is the reference volume, k_B is the Boltzmann constant, ϕ is the polymer volume fraction, N_A is the Avogadro's number, K_{os} is the bulk modulus, ξ is the correlation length, and q is the magnitude of the scattering vector. It is known that the ξ of PNIPA solutions diverges at an MaST temperature with $\xi \sim |T - T_{MaST}|^{-\nu}$, where ν is the critical exponent for ξ. Figure 3 shows OZ plots for PNIPA in D_2O. The solid lines are the fits with Eq. (2). The correlation length diverged at $P \approx 120$ MPa with $\xi \sim |P - P_{MaST}|^{-\nu_P}$. Hence, it was concluded that both temperature and pressure led to a MaST as the correlation length diverges as a critical phenomenon with $\nu \approx 0.5$.

SANS of BC

Figure 4 shows SANS curves of PEOEOVE-*b*-PMOVE ($C = 15$ wt%) in D_2O at various temperatures and at atmospheric pressure ($P = 0.1$ MPa), which show a dramatic increase in the intensity at $T \approx 40.0\,^{\circ}$C.[13] Quantitative analyses of the SANS curves indicate occurrence of MiST with a PEOEOVE core of radius $R \approx 160$ Å in a bcc lattice of $a = 750$ Å. The solid curve is the fit with an OZ function for the data at 20 °C. Different from the *T*-induced phase separation, *P*-induced transition did not accompany MiST, but only a MaST transition occurred with divergence of ξ. The critical exponent in this *P*-induced transition was $\nu \approx 0.61$.

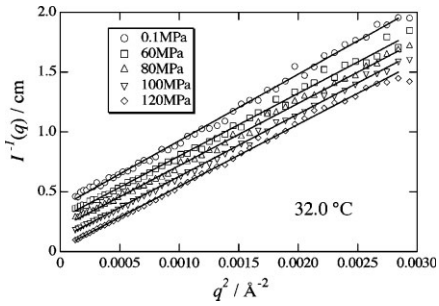

Figure 3.
Ornstein-Zernike plots for the PNIPA solutions at 32 °C.

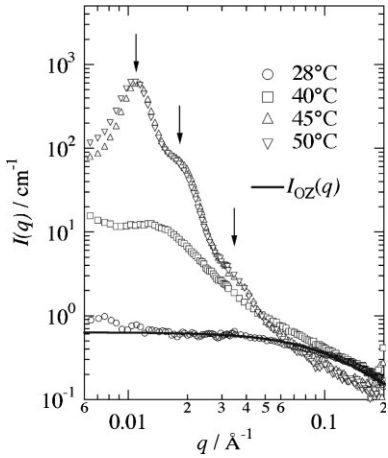

Figure 4.
SANS curves of PEOEOVE*b*-PMOVE in D_2O at various temperatures. $P = 0.1$ MPa.

By extensive SANS studies on PEOEOVE-*b*-PMOVE, we obtained a phase diagram classifying the states of the PEOEOVE-*b*-PMOVE solution. In Figure 5, A, B, and S denote PEOEOVE, PMOVE, and the solvent (D_2O), respectively, and T_1 is the MiST temperature. In region I ($T < T_1$), the system was a homogeneous solution.

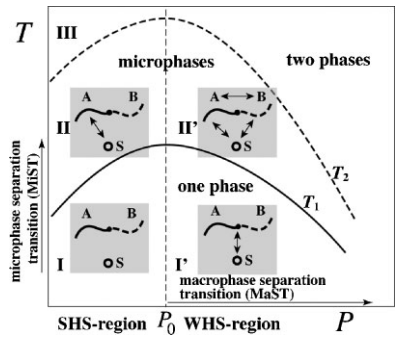

Figure 5.
P-T phase diagram for PEOEOVE-*b*-PMOVE in D_2O. A, B, and S stand for PEOEOVE, PMOVE, and solvent, respectively. The solid and dashed lines denote the T_1 and T_2 curves, respectively. The diagram is divided to several regions, namely, strongly hydrophobic-solvated region (SHS), and weakly hydrophobic-solvated region (WHS), and MiST region.

At low pressures ($P < P_0$), the solution underwent either a MiST at T_1 (region II) or a MaST (precipitation) at T_2 (region III) by increasing T. Each region could be further divided to the strongly hydrophobic-solvated region (SHS; $P < P_0$) and the weakly hydrophobic-solvated region (WHS; $P > P_0$). In the SHS region, hydrophobic solvation was dominant and ΔV_m was negative. On the other hand, the WHS region was characterized by $\Delta V_m > 0$, resulting in the change of the slope of the T_1 curve from positive to negative (from region I to I' or region II to II') at $P = P_0$. From region I to I', concentration fluctuations become large, resulting in a macrophase separation at P_{sp}. The pressure dependence in region II near $T = T_1(P_0)$ is characterized by a reentrant microphase separation as revealed by SANS. Note that the structure in region II' is not highly developed compared with that in region II. This may suggest that the interaction parameter χ in region II' is not as large as that at the symmetric pressure in region II and is a weaker function of T.

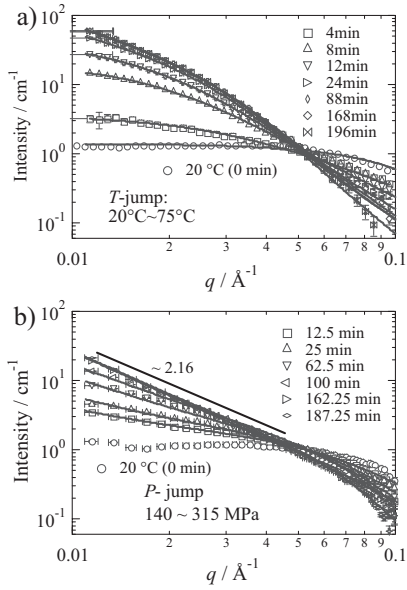

Figure 6.
Evolution of SANS curves of bLG aqueous solutions after (a) *T*- and (b) *P*jumps.

Protein Solution

It was found that the T-induced transition is more specific to the chemical structure of the solute than the P-induced transition. This is why it undergoes a sequential MiST followed by a MaST by increasing temperature. Now, we disucuss the case of protein aqueous solutions, where the solute can be regarded as a multiblock copolymer having different susceptibility against the environment. In the case of protein solutions, heating or pressurization results in an irreversible phase transition. Hence, we discuss structure changes of protein solutions as a function of time after T- or P-jump.

Figure 6a shows a series of the SANS intensity curves, $I(q)$'s, during T-induced gelation under atmospheric pressure. At 20 °C, before starting the T-jump, $I(q)$ (open circles) has a very shallow peak around $q = 0.05$ Å^{-1}, indicating the presence of inter-particle interference at a distance of 125 Å. This SANS profile is successfully fitted with a modified Percus-Yevick equation[14] with a core radius of 23.7 Å and an inter-particle distance of 105 Å. Hence, globular proteins of radius R are packed rather irregularly with a hard core potential. Soon after the T-jump, the SANS intensity began to increase in the low q region, i.e., $q \geq R$. This means that an increase of the concentration fluctuations occurs in the spatial range greater than the size of the globular protein. Coincidentally, the decrease of the SANS intensity in the high q region was observed, which indicated the sharpening of the surface of the particle unit. It should be noted here that no drastic change was observed in the SANS curve in the vicinity of the gelation threshold ($t_g \sim 6$ min) in comparison with dynamic light scattering (DLS) results. After 48 min, no further change was detected within these q ranges (Fig. 6a). We analyzed the SANS intensity curves during T-jump by fitting. In general, the SANS intensity curve, $I(q)$, is given by $I(q) \sim F(q)S(q)$, where $F(q)$ is the form factor representing the shape of the particle and $S(q)$ is the structure factor representing the inter-particle interaction.

Here, we used the $F(q)$ of a hard sphere, which is given by

$$F(q) = \left\{ \frac{3[\sin(qR) - qR\cos(qR)]}{(qR)^3} \right\}^2 \quad (3)$$

where R is the radius of the globular protein. The polydispersity of the sphere size was convoluted in the $F(q)$ as a Gaussian distribution function. Also, we used the Freltoft- Kjems-Sinha function for fractal aggregates as the $S(q)$,[15] which is given by

$$S(q) = 1 + \frac{C(d_f - 1)\Gamma(d_f - 1)\xi^{d_f}}{(1 + q^2\xi^2)^{d_f/2}} \frac{(1 + q^2\xi^2)^{1/2}}{q\xi} \frac{\sin\left[(d_f - 1)\arctan(q\xi)\right]}{d_f - 1} \quad (4)$$

where C is a constant and d_f is the fractal dimension of the aggregate and $\Gamma(x)$ is the gamma function of argument x, and ξ is the correlation length of the aggregate.[15] The scattering curves are well-reproduced by the solid lines as shown in Fig. 6a. At 196 min, R was 73 Å and d_f was 1.40 from the fitting result. The size of R is much larger than the hydrodynamic radius ($R_h = 40$ Å) and the core radius at 20 °C ($R \approx 23.7$ Å). It can therefore be concluded that the particle unit of the gels is an aggregate of a few bLG molecules, i.e., oligomers. This strongly agglutinative aggregation is driven by the hydrophobic interaction of the protein at ambient pressure.[16] $d_f = 1.40$ is smaller than one generally obtained in three dimensions ($2.0 < d_f < 3.0$). However, this result is often observed in other systems too.[17] Furthermore, an ionic strength-dependence of d_f has been observed in a previous study of bLG which provided d_f values lower than 2.0.[18]

Next, we discuss the *P*-induced transition of bLG. Up to 140 MPa, no distinct change of the scattering curves was observed. The stability of bLG against hydrostatic pressure in the low pressure region was also reported by Belloque et al. by NMR.[19] Therefore, we carried out a *P*-jump experiment from 140 to 315 MPa at 20 °C. As shown in Figure 6b, soon after the onset of the *P*-jump, the SANS intensity increased in a different fashion from that in the *T*-jump. Note that the $I(q)$'s are power-law functions of q. The SANS curves could be fitted by Eqs. (3) and (4). After 187.5 min, no significant change of the SANS curve was observed and a power law behavior was observed. In comparison with the *T*-jump, R here is significantly smaller, indicating that the degree of unfolding at the *P*-jump is much less than that of the *T*-jump. On the other hand, the value of d_f increases with time. These results suggest that *P*-denatured gels are formed by fractal aggregates having a large distribution with fine-stranded clusters ($R \approx 40$ Å). *T*-induced denaturation may lead to the unfolding of bLG, followed by the formation of larger globules by the assembly of a few bLG molecules. This results in the formation of dendritic clusters. On the other hand, *P*-induced denaturation promotes partial unfolding and only a few functional groups are activated for the bonding of neighboring bLG molecules. As a result, fine-stranded clusters are formed. This conjecture is consistent with the model discussed by Lopez-Fandino.[19]

Conclusion

T- and *P*-induced phase separation transitions were investigated using small-angle neutron scattering in order to elucidate the *T*- and *P*-effects on phase separation on polymeric systems having different degrees of complexity. In the case of PNIPA aqueous solutions, both *T*- and *P*-induced transitions resulted in a similar MaST. However, in the case of PEOEOVE-*b*-PMOVE block copolymer solutions, a two-step transition, i.e., a MiST followed by a MaST, took place exclusively by increasing temperature, and only a MaST occurred

with increasing *P*. This suggested that hydrophobic interaction is specific at ambient pressure, and hydrophobic interaction becomes nonspecific at high pressures. *P*-induced protein denaturation is also different from *T*-denaturation. A *P*-jump results in a moderate denaturation compared with a *T*-jump and individual protein globules are less unfolded to form fine-stranded self-similar clusters. The weaker hydrophobic interaction with pressurization seems to be common in all three systems investigated in this study.

Acknowledgements: This work was partially supported by the Ministry of Education, Science, Sports and Culture, Japan (Grant-in-Aid for Scientific Research (A), 2006-2008, No. 18205025, and for Scientific Research on Priority Areas, 2006-2010, No. 18068004)).

[1] T. V. Chalikian, K. J. Breslauer, *Biopolymers* **1996**, *39*, 619–626.
[2] W. Kauzmann, *Adv. Protein Chem.* **1959**, *14*, 1; W. Kauzmann, *Nature* **1987**, *325*, 763–764.
[3] S. Sugihara, S. Kanaoka, S. Aoshima, *Macromolecules* **2005**, *38*, 1919–1927.
[4] S. Okabe, M. Nagao, T. Karino, S. Watanabe, T. Adachi, H. Shimizu, M. Shibayama, *J. Appl. Cryst.* **2005**, *38*, 1035–1037.
[5] M. Matsumoto, K. Murakoshi, Y. Wada, S. Yanagida, *Chem. Lett.* **2000**, *29*, 938–939.
[6] M. Shibayama, K. Isono, S. Okabe, T. Karino, M. Nagao, *Macromolecules* **2004**, *37*, 2909–2918.
[7] N. Osaka, M. Shibayama, *Phys. Rev. Lett.* **2006**, *96*, 048303.
[8] A. D. Buckingham, H. G. E. Hentschel, *J. Polym. Sci., Polym. Phys. Ed.* **1980**, *18*, 853.
[9] S. Kunugi, K. Takano, N. Tanaka, *Macromolecules* **1997**, *30*, 4499–4501; N. Tanaka, *Biochim. Biophys. Acta* **2002**, *1595*, 329–344.
[10] I. R. Nasimova, T. Karino, S. Okabe, M. Nagao, M. Shibayama, *Macromolecules* **2004**, *37*, 8721–8729.
[11] S. A. Hawley, *Biochemistry* **1971**, *10*, 2436.
[12] L. Smeller, *Biochim. Biophys. Acta* **2002**, *1595*, 11–1129.
[13] N. Osaka, S. Okabe, T. Karino, Y. Hirabaru, S. Aoshima, M. Shibayama, *Macromolecules* **2006**, *39*, 5875–5884.
[14] M. Shibayama, H. Kawada, T. Kume, T. Sano, T. Matsunaga, N. Osaka, S. Miyazaki, S. Okabe, H. Endo, *J. Chem. Phys.* **2007**, *127*, 144507.
[15] T. Freltoft, J. K. Kjems, S. K. Sinha, *Phys. Rev. B* **1986**, *33*, 269–275.
[16] G. Panick, R. Malessa, R. Winter, *Biochemistry* **1999**, *38*, 6512–6619.
[17] D. A. Weitz, M. Oliveria, *Phys. Rev. Lett.* **1984**, *52*, 1433–1436.
[18] M. Pouzot, T. Nicolai, *Macromolecules* **2004**, *37*, 614–620.
[19] J. Belloque, G. M. Smith, *J. Agric. Food Chem.* **2000**, *48*, 3906–3912; J. Belloque, R. Chicon, L.-F. R, *J. Agric. Food Chem.* **2007**, *55*, 5282–5288; R. Lopez-Fandino, *Crit. Rev. Food. Sci. Nutr.* **2006**, *46*, 351–363.

